Toxicology 410 (2018) 171–181

Contents lists available at ScienceDirect

Toxicology

journal homepage: www.elsevier.com/locate/toxicol

Evaluation of non-invasive biomonitoring of 2,4-Dichlorophenoxyacetic acid (2,4-D) in saliva

Zana A. Carver[1], Alice A. Han, Charles Timchalk, Thomas J. Weber, Kimberly J. Tyrrell, Ryan L. Sontag, Teresa Luders, William B. Chrisler, Karl K. Weitz, Jordan N. Smith*

Chemical Biological & Exposure Science Team, Pacific Northwest National Laboratory, Richland, WA 99352, United States

ARTICLE INFO

Keywords:
2,4-Dichlorophenoxyacetic acid
Biomonitoring
Biological modeling
Exposure assessment
In vitro and alternatives

ABSTRACT

The objective of this study was to evaluate the potential for non-invasive biomonitoring of 2,4-Dichlorophenoxyacetic acid (2,4-D) in saliva. Using an *in vitro* rat salivary gland epithelial cell (SGEC) system, a collection of experiments investigating chemical protein binding, temporal and directional transport, as well as competitive transport with para-aminohippuric acid (PAH), a substrate for renal organic anion transporters, was conducted to identify cellular transport parameters required to computationally model salivary transport of 2,4-D. Additionally, a physiological protein gradient was implemented to mimic physiologically relevant concentrations of protein in rat plasma and saliva, and under these conditions the transfer of 2,4-D was markedly slower, driven by increased protein binding (*i.e.* reduced free 2,4-D species available to cross salivary barrier). The rate of transfer was directly proportional to the amount of unbound 2,4-D and demonstrated no indication of active transport. An *in vivo* assessment of 2,4-D exposure in rats revealed non-linear protein binding in plasma, indicating saturated protein binding and increased levels of unbound 2,4-D species at higher doses. A strong correlation between 2,4-D concentrations in saliva and unbound 2,4-D in plasma was observed (Pearson correlation coefficient = 0.95). Saliva:plasma 2,4-D ratios measured *in vivo* (0.0079) were consistent within the linear protein binding range and expected 2,4-D levels from occupational exposures but were significantly different than ratios measured *in vitro* (physiological conditions) (0.034), possibly due to 2,4-D concentrations in saliva not being at equilibrium with 2,4-D concentrations in blood, as well as physiological features absent in *in vitro* settings (*e.g.* blood flow). We demonstrated that 2,4-D is consistently transported into saliva using both *in vitro* and *in vivo* models, making 2,4-D a potential candidate for human non-invasive salivary biomonitoring. Further work is needed to understand whether current sensor limits of detection are sufficient to measure occupationally relevant exposures.

1. Introduction

2,4-Dichlorophenoxyacetic acid (2,4-D) is a commonly used, broad-leaf selective herbicide. Acting as an auxin agonist, 2,4-D causes uncontrolled growth and eventual death in various broad-leaf species (Garabrant and Philbert, 2002; Kennepohl et al., 2010). In 2012, 2,4-D was the 5th most used herbicide for agriculture (30–40 million pounds), as well as the favored choice in the home and garden (7–9 million pounds) across the United States (US EPA, 2017a). Due to the substantial reliance and application of 2,4-D, there is concern regarding the risks of human exposure, which can occur directly during manufacturing, mixing, loading, and applying processes of the herbicide, or indirectly by inhabiting shared spaces with those involved in routine handling of 2,4-D (Aylward et al., 2010). Oral ingestion, inhalation and dermal absorption are typical routes of exposure, with chemical deposition on the skin being a large contributor (80–90%) of potential exposure (Grover et al., 1986).

Considerable assessments of possible adverse effects of 2,4-D exposure have been conducted, investigating genotoxicity, reproductive toxicity, cancer, and neurotoxicity in animal models and humans. Notably, 2,4-D doses ≥ 50 mg/kg in rats appear to have a widespread impact, ranging from renal tubule damage (Charles et al., 1996) to central nervous system toxicity (Munro et al., 1992). Exposure to 2,4-D in humans have also been associated with non-Hodgkins lymphoma in epidemiological studies (Hoar et al., 1986;

* Corresponding author at: P.O. Box 999, Richland, WA, United States.
E-mail address: Jordan.Smith@pnnl.gov (J.N. Smith).
[1] Present address: Department of Biology, Columbia Basin College, Pasco, WA 99301, United States.

https://doi.org/10.1016/j.tox.2018.08.003
Received 5 June 2018; Received in revised form 1 August 2018; Accepted 9 August 2018
Available online 16 August 2018
0300-483X/

Zahm et al., 1990); however, major reviews conclude that the weight of evidence does not support a causal relationship (Burns and Swaen, 2012; Garabrant and Philbert, 2002; Goodman et al., 2015; Von Stackelberg, 2013). Most epidemiological studies with larger sample sizes (over 200 cases) lack consistent statistical associations, while some investigations with either small sample sizes (< 200 cases) or poor estimates of exposure (duration proxy, questionnaires) report positive associations of 2,4-D and non-Hodgkins lymphoma (Burns and Swaen, 2012; Garabrant and Philbert, 2002; von Stackelberg, 2013). A general lack of 2,4-D biomonitoring data, specifically with larger epidemiological studies, has significantly contributed to inconsistent conclusions regarding 2,4-D carcinogenicity and has possibly even resulted in misclassification of 2,4-D carcinogenic potential (Burns and Swaen, 2012; Goodman et al., 2015). Biomonitoring measurements for both large and small epidemiology investigations would reduce inconsistencies and allow for a more meaningful interpretation of epidemiological data.

2,4-D is eliminated by renal excretion *via* glomerular filtration and active transport by organic anion transporters (OATs) in the renal tubules (Villalobos et al., 1996). With a half-life of 10–33 h (of the parent compound) measured in human urine (Sauerhoff et al., 1977), urine serves as a favorable biomonitoring matrix for 2,4-D (Burns and Swaen, 2012; Aylward et al., 2013) and has been used to establish biomonitoring equivalent (BE) levels of 2000 μg/L (urine) (Aylward and Hays, 2008). Although 24 h urinary collections provide robust data regarding total 2,4-D exposures, it is difficult to correlate 2,4-D amounts excreted in urine to 2,4-D concentrations in blood or other target tissue concentrations (Arcury et al., 2006; Ferrari et al., 2008; Smolders et al., 2009; Aylward and Hays, 2008; Aylward et al., 2010). Additionally, urine collections are often hampered by a lack of participant cooperation and missing samples. Spot urine samples are easier to collect, however, suffer from volume and concentration variation. Creatinine adjustments are often applied to correct for volume variability, but creatinine levels can vary according to gender, age, and weight-to-height ratio (Aylward and Hays, 2008). As such, 24 h urinary collections provide useful measurements of 2,4-D exposure, but other approaches may be more valuable for blood or target tissue dosimetry.

One potential alternative matrix to urine for non-invasive biomonitoring is saliva. Saliva is both easily sampled, cost effective, and has been widely utilized to measure drugs, heavy metals, hormones, and metabolites (Esteban and Castano, 2009; Kaufman and Lamster, 2002). Many chemicals are measured in saliva at slightly lower but comparable levels to blood and urine (Jusko and Milsap, 1993; Michalke et al., 2015; Silva et al., 2005). It must also be noted that urine measures total exposures over a specific time interval, while blood concentrations may be very different during these intervals (Ferrari et al., 2008; Lu, 2006). This discrepancy may be significant for seasonal pesticides with a short half-life and repeated saliva measurements may give a better indication of blood and tissue exposure levels over time. Furthermore, non-ionized and lipophilic chemicals with a lower affinity for plasma proteins demonstrate consistently high partitioning into saliva; however, less is known about plasma to saliva partitioning of ionized or highly protein-bound chemicals.

The objective of this study was to evaluate the potential for non-invasive biomonitoring of 2,4-D in saliva. Previously, our group utilized an *in vitro* rat salivary gland epithelial cell (SGEC) system coupled with computational modeling to successfully predict *in vivo* salivary transport of a chlorpyrifos metabolite 3,5,6-trichloro-2-pyridinol (TCPy) (Smith et al., 2017; Timchalk et al., 2015; Weber et al., 2017). Here, the SGEC model system was applied to 2,4-D to understand mechanistic aspects of salivary transport and to predict *in vivo* salivary transport. Finally, predictions from the SGEC system were compared to measured 2,4-D concentrations in plasma and saliva of rats dosed orally with 2,4-D.

2. Materials and methods

2.1. Chemicals

2,4-Dichlorophenoxyacetic acid (2,4-D) (CAS no. 94-75-7), para-aminohippuric acid (PAH) (CAS no. 61-78-9), triclopyr (CAS no. 55335-06-3), trimethylsilyldiazomethane (TMSD) (CAS no. 18107-18-1), *N*-tert-Butyldimethylsilyl-*N*-methyltrifluoroacetamide (MTBSTFA) (CAS no. 77377-52-7), ethyl acetate, toluene, lucifer yellow, pilocarpine, and other general laboratory chemicals were purchased from Sigma-Aldrich (St. Louis, MO, USA). Anti-CRB3 rat primary monoclonal antibody was purchased from MyBioSource (Cat # MBS588104) and goat anti-rat IgG secondary antibody-Alexa Fluor 488 conjugate was purchased from Invitrogen (Cat # A11006).

2.2. Animals

Male Sprague-Dawley rats (250–350 g) were purchased from Charles River Laboratories, Inc. (Raleigh, NC). Adult rats were housed in accordance with the National Research Council Guidelines and all experimental protocols were reviewed by the Institutional Animal Care and Use Committee of Battelle, Pacific Northwest Division. Feed (PMI 5002, Certified Rodent Diet) and water were provided *ad libitum*, except feed was withdrawn overnight before dosing.

2.3. Cell culture

Primary SGECs were used to evaluate 2,4-D transport mechanisms and quantify relevant transport parameters. SGECs were isolated from the submaxillary gland of adult male Sprague-Dawley rats and were cultured as previously described (Weber et al., 2017). Briefly, cells were cultured in Advanced DMEM:F12 supplemented with 2% FBS, 10 ng/ml epidermal growth factor (EGF), 2 mM GlutaMAX, 100 U/ml penicillin, 100 U/ml streptomycin, and 0.25 μg/ml Fungizone. Cells were sub-cultured by trypsinization.

2.4. Cellular polarity

Polarity of SGECs was measured using confocal microscopy to identify the Crumbs apical polarity complex (CRB3), a highly conserved protein complex found on apical sides of polarized epithelial cells (Bulgakova and Knust, 2009; Aijaz et al., 2006). Prior to imaging, specificity of the primary antibody was checked with western blot separation and immunoblot analysis along with actin (EMD Millipore, Billerica, MA) as a positive control and proved to be specific for one epitope within the expected molecular weight range. Due to the low molecular weight of CRB3(~10 kDa), glutaraldehyde crosslinking of proteins to the PVDF membrane was required prior to western blot analysis.

In situ analysis of CRB3 by confocal and/or epifluorescence microscopy was performed as previously described (Weber et al., 2017). SGECs were fixed with 3.6% paraformaldehyde + 0.024% saponin for 12 min at room temperature and then permeabilized with PBS + 0.2% Triton X-100 for 5 min, with gentle rocking. Cells were blocked in PBS + 2% bovine serum albumin (BSA) and 5% goat serum for 1 h at room temperature. Incubation with primary anti-CRB3 antibody (1:1000) was performed for 1 h at room temperature. After washing with PBS + 2% BSA, cells were incubated with a goat anti-rat secondary antibody (1:5000) conjugated to $Alexa_{488}$ for 1 h at room temperature. Nuclei were stained with 4′,6-diamidino-2-phenylindole (DAPI). Secondary antibody alone controls were included in all experiments at equal exposure times and showed no detectable signal (data not shown). Microscopic images were acquired on a Zeiss LSM 710 Scanning Confocal Laser Microscope (Carl Zeiss MicroImaging GmbH, Jena, Germany) equipped with a Plan-Apochromat 63x/1.40 Oil DIC M27 objective. The $Alexa_{488}$ secondary antibody was excited at

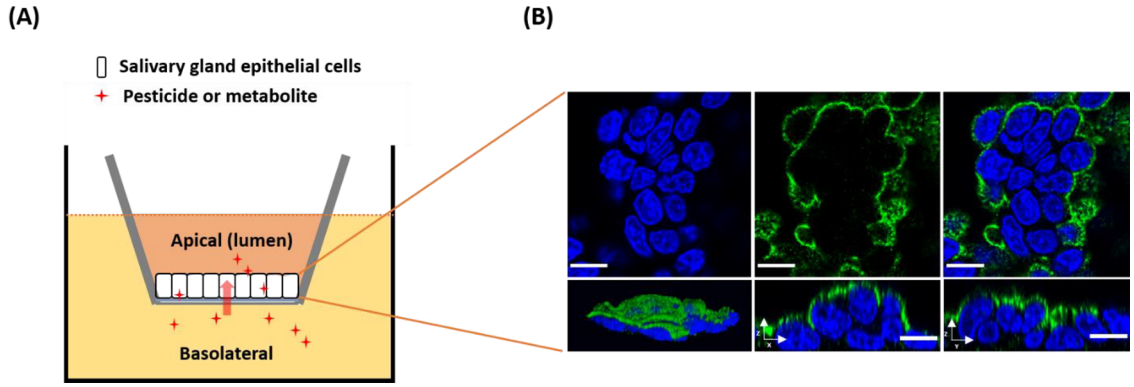

Fig. 1. Transwell system with serous-acinar cells grown on a Transwell insert that separates the apical (saliva) and basolateral (plasma) compartments (A). Confocal microscopy of SGECs grown on Nunc Tech II chamber slides 6 days post-seeding (B). DAPI (nuclear stain) shown in blue (top left) and Crumbs apical marker of polarity (CRB3) in green (top center). Overlay of nuclear stain and CRB3 (top right), 3-D rendering (bottom left), cross-sectional x–z axis (bottom center), and cross-sectional y–z axis (bottom right) identify CRB3 localization on the apical surface of SGECs. Scale bar = 10 μm (For interpretation of the references to colour in this figure legend, the reader is referred to the web version of this article).

488 nm and visualized at 494–630 nm. DAPI stained nuclei were excited at 405 nm and measured at 410–503 nm. Images were processed with Volocity (Perkin Elmer, Waltham, MA, USA) or Zen/Image J software (Molecular Devices, Sunnyvale, CA).

2.5. Tight junction formation

SGEC barrier function was evaluated using transepithelial electrical resistance (TEER) and lucifer yellow (LY) permeability tests as previously described (Weber et al., 2017). Briefly, SGECs were seeded on Falcon® Transwell cell culture inserts (see Fig. 1A; catalog #353092; 3 μm pore, 2.0 ± 0.2 × 10^6 pores/cm^2, 4.2 cm^2 effective growth area, 6 well format). TEER measurements were obtained with the EVOM ^{2} epithelial voltohmmeter and 4 mm double chopstick electrodes (World Precision Instruments, Sarasota, FL, USA). TEER values greater than 200 Ω (840 Ω × cm^2) were indicative of adequate barrier function. An additional control for tight junction formation employed LY transport, which essentially does not pass across epithelial barriers with established tight junctions (Hidalgo et al., 1989; Weber et al., 2017). Adequate TEER correlated experimentally with less than 2% LY passage across the epithelial barrier per hour (Weber et al., 2017).

2.6. Protein binding

Levels of 2,4-D binding to protein were measured in non-physiological (2% FBS in Advanced DMEM:F12) and in physiological media (2% FBS Advanced DMEM:F12 with added BSA to match plasma and saliva protein concentrations in rats). 2,4-D was spiked into non-physiological (1.8 mg/ml protein) media at 10 different concentrations (20–2200 μM) and in physiological (70.6 mg/ml protein) media at 5 different concentrations (50–2200 μM). Protein concentrations were measured using the bicinchoninic acid assay (BCA) with BSA as an external standard. Samples were incubated at 37 °C for 1 h, and aliquots of each sample were transferred to Amicon Ultra Centrifugal Filters (with a 10 kDa cutoff). Samples were then centrifuged at 14,000 RCF x g for 20 min. 2,4-D concentrations were quantified from both the filtered (unbound) and unfiltered (total) samples using the analytical protocol (*2,4-D Quantification*). After samples were quantified, bound 2,4-D concentration was calculated by the difference in concentration of the total (bound + unbound) samples and unbound (filtered) samples. The bound concentration (C_b) of 2,4-D was evaluated as a function of the unbound concentration (C_u) of 2,4-D using a non-linear model. The model assumes one binding site (Eq. (1)) rather than two binding sites (Eq. (2)), where B_{max} is the maximum number of binding sites and k_d is the affinity constant. Optimization of the model used a maximum likelihood objective and the Bayesian information criterion (BIC) to determine the best-fit model (Smith et al., 2017). B_{max} values were scaled to protein concentrations measured in non-physiological and physiological media.

$$C_b = \frac{Bmax \times C_u}{k_d + C_u} \quad (1)$$

$$C_b = \frac{Bmax_1 \times C_u}{k_{d1} + C_u} + \frac{Bmax_2 \times C_u}{k_{d2} + C_u} \quad (2)$$

2.7. Non-physiological transport experiments

2,4-D cellular transport was evaluated with SGECs under non-physiological conditions from the basolateral chamber to apical chamber. SGECs were seeded and grown on Transwell inserts until optimal tight junction integrity was reached. Standard growth media (as described in *Cell Culture*) was changed prior to experiments, but due to a transient disruption of tight junctions with media replacement (Weber et al., 2017), cells were allowed to equilibrate for at least 1 h following the media exchange. The dose receiving chamber was supplemented with 1 mL media, while the contralateral compartment received 2 mL media. This allowed for the addition of 1 ml of a 2× concentration dosing solution to the dose receiving chamber without disrupting tight junctions. Final volumes (2 mL) in both compartments were kept consistent for all transport experiments and final dose concentrations ranged from 45.2 μM to 457 μM. 2,4-D transport from apical to basolateral compartments, or *vice versa*, was evaluated by sampling media at different time points (2, 4, 6, 8, 24 h) from both compartments.

A subsequent competitive transport assay was conducted to assess the contribution of organic anion transporters to 2,4-D transport. Para-aminohippuric acid (PAH), a substrate for renal organic anion transporters, was used as a competitive inhibitor of organic anion transport. PAH (0, 0.1, 1, 10 μM) was co-dosed with 2,4-D (45.2 μM) in only the basolateral chamber. 2,4-D concentrations were measured in the apical compartment 4 h post-dose.

2.8. Physiological transport experiments

2,4-D cellular transport under physiological conditions was evaluated with SGECs. Similar to non-physiological media, physiological media utilized Advanced DMEM:F12 with 2% FBS but also contained 70.6 mg/mL BSA in the basolateral chamber (plasma surrogate) and 2.2 mg/mL BSA in the apical chamber (saliva surrogate). All other experimental conditions (as described in *Non-Physiological Transport Experiments*) were consistent between experiments so that the effect of adding a physiological protein gradient between the basolateral and

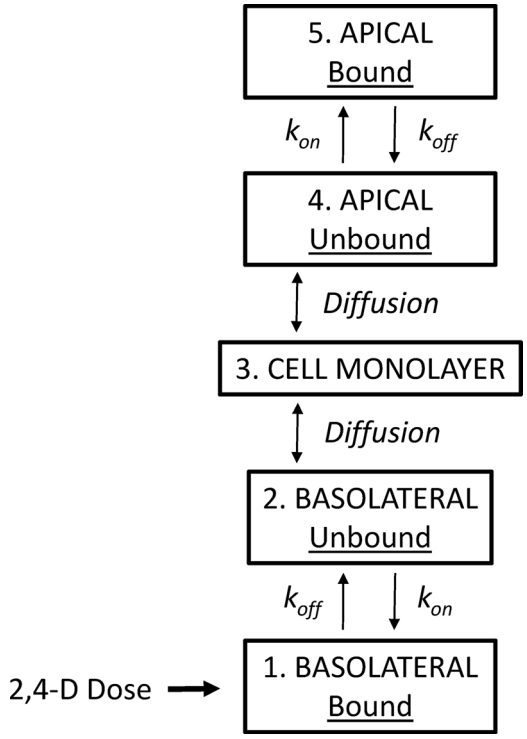

Fig. 2. A schematic of the SGEC system that assumes Fick's diffusion of unbound 2,4-D species (adapted from Smith et al., 2017). A five compartment model comprised of bound (1) and unbound (2) 2,4-D in basolateral compartments transported through the cell monolayer (3) to the apical unbound (4) and bound (5) compartments. Bound and unbound protein populations are driven by k_{on}/k_{off} and unbound species are diffused between apical and basolateral compartments through the cell monolayer.

apical compartments could be accurately assessed. Basolateral chambers were dosed with final 2,4-D concentrations of 67 μM and 284 μM. Media from both apical and basolateral compartments were collected at 2, 4, 6, 8, 24, and 32 h post-dose. It was hypothesized that the rate of 2,4-D transport would be markedly slower under physiological protein gradient conditions due to an increased degree of protein binding. Accordingly, total exposure durations were extended from 24 to 32 h.

2.9. In vivo experiments

Salivary transport of 2,4-D was measured *in vivo* using Sprague-Dawley rats as an animal model. Rats (n = 3 per group) were dosed with 5 different concentrations (30, 44, 67, 100, and 150 2,4-D mg/kg), for a total of 15 rats. Rats were dosed with 2,4-D prepared in phosphate buffered saline with 10% Tween 20, delivered by oral gavage. Approximately 40 min after dosing, rats were anesthetized through intraperitoneal (IP) injection of 87:13 mg/ml ketamine:xylazine. After anesthesia (~10 min), rats were administered 1 mg/ml pilocarpine *via* IP injection to induce salivation (Smith et al., 2010, 2012). Oral fluid was collected gravimetrically for 10 min from the oral cavity using a 9.52 cm × 2.49 o.d. × 1.42 i.d. glass capillary tube passively placed in the corner of the mouth, draining into a 2 mL microcentrifuge collection vial. While the term "oral fluid" describes a mixture of saliva from multiple glands, cellular debris, electrolytes, proteins, antibodies, other exogenous substances (Carpenter, 2013; Humphrey and Williamson, 2001), the term "saliva" is often used in literature to reflect oral fluid samples in the context of biomonitoring (Michalke et al., 2015; Lew et al., 2010; Staff et al., 2014; Smolders et al., 2009; Caporossi et al., 2010). "Saliva" is used throughout this work in reference to oral fluid collected from animals. After saliva was collected, rats were immediately euthanized by CO_2 inhalation from a compressed gas cylinder, followed by cervical dislocation. Terminal blood was collected by cardiac puncture and exsanguination and blood was drawn into a syringe loaded with 10 μL 1000 U/mL heparin. An aliquot of whole blood was immediately centrifuged at 1600 × *g* for 10 min to extract plasma. Bound and unbound protein levels in plasma were quantified with methods previously described in *Protein binding*. All samples were kept frozen in liquid nitrogen until they were analyzed, as detailed in *2,4-D quantification*. Sample collection times corresponded to approximately 1 h of total exposure.

2.10. 2,4-D quantification

2,4-D was measured in cell culture medium, cells, plasma, and saliva using gas chromatography-mass spectrometry (GC–MS). Triclopyr was added to each sample as an internal standard. Samples were acidified by adding 3 M HCl saturated with NaCl and extracted twice with ethyl acetate. Samples were dried with Na_2SO_4, and ethyl acetate was gently evaporated under a gentle stream of nitrogen. Samples were reconstituted in toluene (1 mL) and derivatized with MTBSTFA. These samples were analyzed by negative ion chemical ionization by GC–MS, as performed in Smith et al. (2012). For samples of low concentrations (physiological *in vitro* and *in vivo* experiments), an alternative derivatization method was needed for increased sensitivity (Moy and Brumley, 2003; Ranz et al., 2008). In this method, samples were reconstituted with 120 μL of toluene and 80 μL of methanol and derivatized with 20 μL of dimethylsilydiazomethane (TMSD) to yield methyl esters of 2,4-D and Triclopyr. Derivatized samples were then analyzed with a Hewlett-Packard (Palo Alto, CA) 5973 mass selective detector, ChemStation data analysis (6890 N), and a Rtx-1701 30 m × 0.25 mm id × 0.25 μm df column (Bellefonte, PA, USA). Helium was used as the carrier gas at a pressure of 24 psi with an initial oven temperature of 100 °C and inlet temperature of 210 °C. The oven temperature was ramped 20 °C/min to 120°, then ramped 10 °C/min to 260 °C, and held for 10 min. Silylated derivatives (using MTBSTFA) and methyl esters (using TMSD) of 2,4-D and triclopyr were detected with selective ion monitoring (SIM) of the quantifiable ions 142 *m/z* and 219 *m/z*, and 234 *m/z* and 273 *m/z*, respectively. This method resulted in an LOD = 1.7 ng/ml (ppb) and LOQ = 5.1 ng/ml. 2,4-D concentrations were quantified with external 2,4-D calibration standard curves prepared in cell culture medium, cells, plasma, or saliva.

2.11. Computational modeling

A cellular computational model describing simple passive diffusion in the Transwell system (Smith et al., 2017) was modified for 2,4-D transport. For cellular transport experiments, a five compartment model incorporating unbound 2,4-D transport among the apical (saliva), cellular (monolayer), and basolateral (plasma) chambers was established (Fig. 2). Since there was no indication of active transport, differential equations for passive diffusion utilizing Fick's Law were used to describe diffusional transport among apical (A), cell (C), and basolateral (B) compartments, where t is time (h), A is the amount (nmol) of 2,4-D, SA is the surface area of cells (cm^2), PA is the permeability coefficient (cm/h), P is the partition coefficient, and C is the concentration (μmol/L) (Eqs. (3)–(5)). The permeability coefficient is the product of the cell membrane thickness (cm) and the diffusion coefficient (cm^2/h). Concentrations were calculated by normalizing amount to volume, and amount by integrating the differential rate equation for each compartment, as performed in Smith et al. (2017).

$$\frac{dA_A}{dt} = -PA_{AC}\, x\, SA_C\, x \left(C_A - \frac{C_C}{P_{CA}}\right) \tag{3}$$

$$\frac{dA_C}{dt} = Pa_{AC} x SA_C x \left(C_A - \frac{C_C}{P_{CA}}\right) + PA_{BC} x SA_C x \left(C_B - \frac{C_C}{P_{CB}}\right) \tag{4}$$

Table 1
Cellular transport parameters used in the *in vitro* computational transport model for both non-physiological and physiological experiments, and *in vivo* saliva/plasma ratios.

Parameter	Value	References
Protein Concentrations		
Non-physiological medium (mg/mL)	1.8	Measured
Physiological plasma surrogate medium (mg/mL)	70.6	Measured
Physiological saliva surrogate medium (mg/mL)	2.2	Measured
Protein-binding Parameters		
Bmax for non-physiological (nmol/mg protein)	90.5	Measured[a]
Kd for non-physiological (μM)	926.1	Measured
Bmax for physiological – plasma (nmol/mg protein)	51.5	Measured[a]
Bmax for physiological – saliva (nmol/mg protein)	74	Measured[a]
Kd for physiological (μM)	67	Measured
Kon (1/M/s)	1×10^6	Estimated (Mironov et al., 2011; Smith et al., 2017)
Volumes		
Cells (mL)	0.0022	Estimated (2×10^6 cells) × (1100 μm^3/cell) (Smith et al., 2017)
apical chamber (mL)	2	Set experimentally (Weber et al., 2017)
basolateral chamber (mL)	2	Set experimentally (Weber et al., 2017)
Cell Parameters		
Effective Surface area (cm^2)	4.2	Effective growth area of Transwell
Permeation coefficient (cm/h)	0.033	Optimized
Partition coefficient (unitless)	4.45	Measured
Saliva/Plasma Ratio (unitless)		
in vitro	0.034	Measured
in vivo	0.0079	Measured

[a] Bmax values normalized to protein concentration.

$$\frac{dA_B}{dt} = -PA_{BC}\ x\ SA_C\ x \left(C_B - \frac{C_C}{P_{CB}}\right) \quad (5)$$

2.12. Parameterization

Parameters in the cellular computational model were set according to experimental data and literature values (Table 1). Protein binding parameters were measured as described in the *Protein binding* section. Volumes associated with each chamber were experimentally set or estimated from literature sources. The partition coefficient was determined with experimental data of 2,4-D (457 μM) equilibration under non-physiological conditions. The permeation coefficient was optimized to 2,4-D concentrations measured in non-physiological media from apical and basolateral chambers following 2,4-D (457 μM) transport across the cellular monolayer. Optimization employed a Conjugate Gradient algorithm with a heteroscedasticity value of 1.0.

2.13. Sensitivity analysis

Sensitivity analyses were conducted to evaluate parameter importance in predicting 2,4-D concentrations using the *in vitro* cellular computational model. Normalized sensitivity coefficients were calculated for a 1% change of a given parameter, while holding all other parameters constant. Parameter sensitivity was determined under non-physiological and physiological conditions, where the basolateral (plasma) chamber received the dose (60 μM (non-physiological) or 67 μM (physiological) 2,4-D), and the chemical is transported into the apical (saliva) chamber. The following parameters were assessed: partition coefficient, permeability coefficient, Bmax (number of binding sites) in both apical and basolateral chambers, and K_d (affinity constant) in both apical and basolateral chambers.

2.14. Statistical analysis

Statistical analysis of data was conducted with R: A language and environment for statistical computing, version 3.3.1, 3.3.2, 3.3.3, and 3.4.3 (R Foundation for Statistical Computing, Vienna Austria) and Minitab 17.3.1 (Minitab Inc., State College, PA USA) using Welch's and Fisher's t-test, or ANOVA as appropriate, considering $p < 0.05$ as significant. The cellular computational model was coded in acslX 3.1.4.2 (Aegis Technology, Huntsville, AL USA).

3. Results

3.1. Monolayer integrity

SGECs maintained tight junctions throughout transport experiments. All experimental TEER values (pre-dose and post-dose) were ≥ 1156 Ω*cm^2. On average, TEER values increased ~ 17.5% from pre-dose to final sample collection. In addition, lucifer yellow (20 μg/ml) passage across SGEC monolayers during experiments was minimal (≤ 0.22%/h and ≤ 0.06%/h for non-physiological and physiological experiments, respectively). These values were sustained over the course of each experiment, demonstrating reasonable tight junction integrity.

3.2. Protein binding

2,4-D bound reversibly to proteins in both non-physiological and physiological media. Within the range of 20–2200 μM, 2,4-D displayed a dissociation constant (Kd) of 926.1 μM and a maximum binding capacity (Bmax) of 90.5 nmol/mg protein (normalized to 1.8 mg/mL protein content) in non-physiological media (Fig. 3A). In physiological media, at the concentration range of 50–2200 μM 2,4-D, a dissociation constant (Kd) of 67.0 μM (higher affinity compared to non-physiological media) was determined. Bmax values of 51.5 nmol/mg protein (normalized to 70.6 mg/mL protein content (plasma)) and 74.04 nmol/mg protein (normalized to 2.2 mg/mL protein content (saliva)) were determined (Fig. 3B). For all conditions, a one binding site model (Eq. (1)) provided the best fit, compared to a 2 binding site model (Eq. (2)) (BIC = 85.9 *vs* 90.8 – non-physiological; BIC = 65.4 *vs* 68.6 – physiological). This suggests that one apparent binding site was dominant for these assays. Fractions of bound 2,4-D ranged from 0.051 – 0.41 in non-physiological conditions and 0.96 - 0.99 in physiological conditions over selected concentrations used in these experiments.

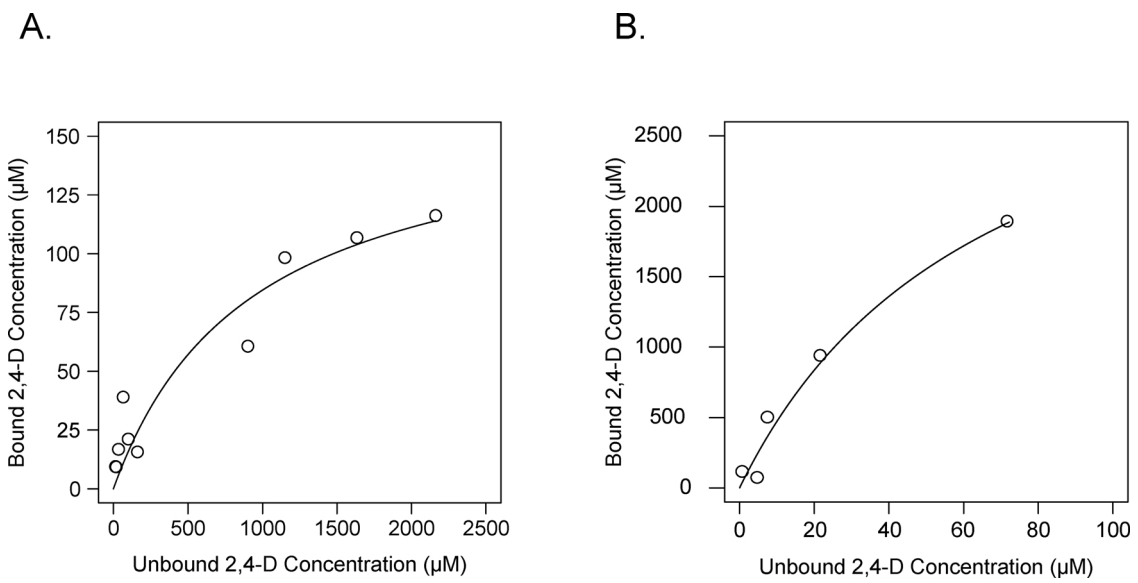

Fig. 3. Concentrations of 2,4-D bound and unbound to proteins in non-physiological cell culture medium (A) and physiological medium (B). Lines are resulting fits to a one binding site model (Eq. (1)).

3.3. SGEC polarity

CRB3, with expected apical localization, was used to assess SGEC polarity by confocal microscopy. As shown in Fig. 1B, strong apical staining of CRB3 was observed with no CRB3 detection basolaterally. This observation suggests that SGECs form polarized monolayers *in vitro*, which may be an important feature of regulating transport mechanisms.

3.4. Transport in non-physiological conditions

Directional transport experiments and co-transport experiments with PAH did not exhibit evidence of active transport mechanisms. The directional transport experiment demonstrated equivalent concentrations in each chamber at 4 and 24 h after dosing (42.5 μM or 240 μM), regardless of the direction of transfer (apical to basolateral and *vice versa*) ($p = 0.813$) (Fig. 4A). Additionally, a competitive substrate experiment of 2,4-D with para-aminohippuric acid (PAH), a known OAT substrate, demonstrated no significant difference in 2,4-D transport (basolateral to apical) among the four concentrations of PAH ($p = 0.411$) (Fig. 4B).

Non-physiological (standard media) transport experiments without a protein gradient provided further evidence of diffusional transport. In a 24 h time-course experiment (basolateral to apical transfer), 2,4-D demonstrated transport to equilibrium across the monolayer resulting in equivalent concentrations in both compartments ($p = 0.926$) at 24 h after dosing (60 μM or 457 μM) (Fig. 5A and B). Initial transfer of 2,4-D from basolateral to apical compartments was rapid and allowed GC–MS detection at 2 h time-points. The pH of the media in compartments did not vary from the 7.2–7.6 range. The mass balance indicated a slight loss from the system (~10%) at the 2 h time-points that was not recovered at later time-points and not explained by the negligible amount of 2,4-D measured in the cells at 24 h. Loss of mass may be due to dilution of the receiving apical chamber, in which a slight amount of

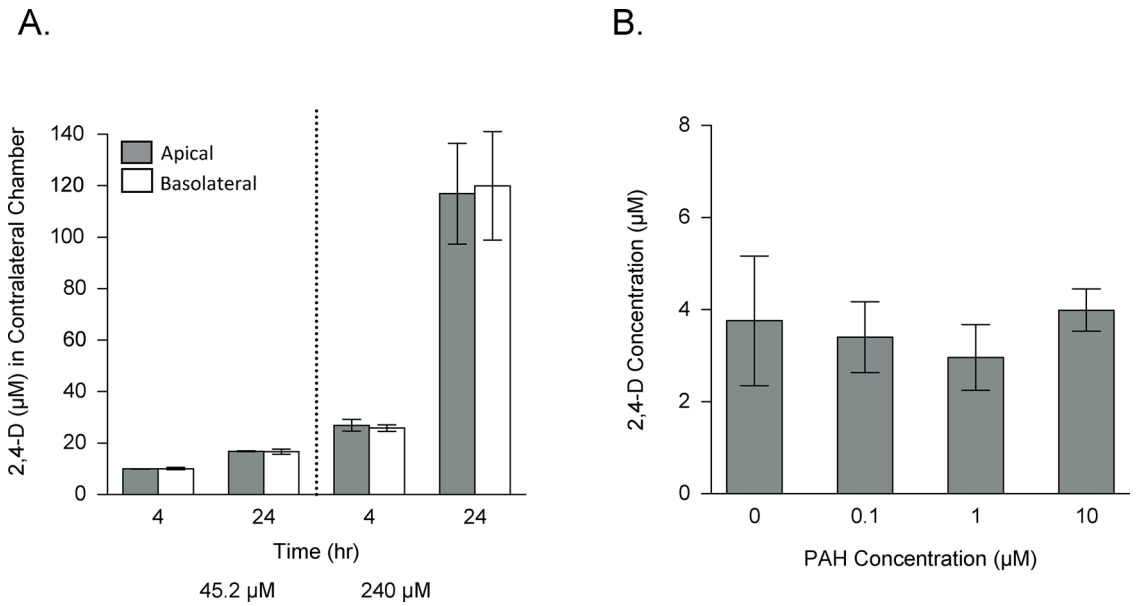

Fig. 4. 2,4-D concentrations in the contralateral chamber after 4 and 24 h dosing 45.2 or 240 μM of 2,4-D in the apical (gray) or basolateral (white) chamber (A). 2,4-D concentrations in the apical chamber 4 h after co-dosing the basolateral chamber with 45.2 μM 2,4-D and 0, 0.1, 1, or 10 μM of para-aminohippuric acid (PAH) (B).

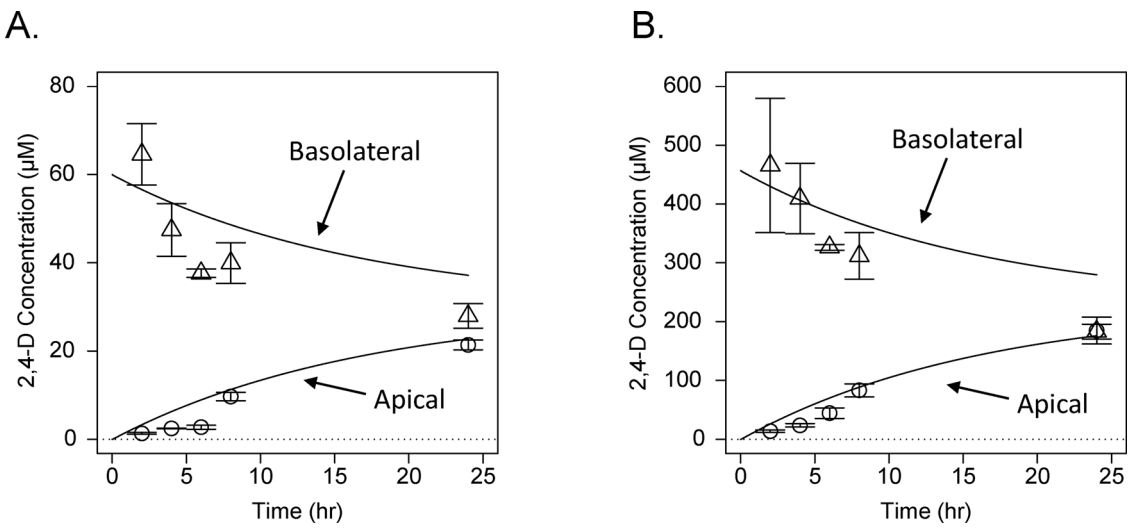

Fig. 5. Concentrations of 2,4-D in cell culture medium in basolateral (triangles) and apical (circles) chambers over time (24 h) following 60 μM (A) or 457 μM (B) 2,4-D dosed in the basolateral chamber under non-physiological experimental conditions. Lines are computational model simulations fit to the data. The dotted line is the LOQ.

media is left to prevent cells from detaching during media changes, potentially creating a slightly greater volume and an apparent loss of 2,4-D. Equivalent concentrations in apical and basolateral compartments at equilibrium suggested that passive diffusion is the primary transport mechanism under these conditions. 2,4-D demonstrated dose-dependent times to reach equilibrium, of 24 h for the 60 μM and 22 h for the 457 μM dose. The measured unbound fractions that are able to transverse the SGEC monolayer, 0.86 and 0.89 (for the doses of 60 and 457 μM) corresponded with the equilibrium times.

After parameterization, the cellular computational model was able to accurately predict non-physiological transport of 2,4-D. Partitioning of 2,4-D between the cell/apical and cell/basolateral at 24 h (non-physiological) was measured at equilibrium. A partition coefficient of 4.45 was used to computationally model 2,4-D transport in both non-physiological and physiological media. The permeation coefficient was optimized to 2,4-D concentrations in both chambers following a 457 μM dose under non-physiological conditions. The optimized permeation coefficient of 0.033 cm/h was also able to reasonably predict the transfer of 2,4-D at the lower dose (60 μM), thus validating the permeation coefficient. The cellular computational model, parameterized with protein binding constants, predicted dose-dependent times to reach equilibrium (Fig. 5A and B).

3.5. Transport in physiological (protein gradient) conditions

A protein gradient of basolateral/plasma (70.6 mg BSA) and apical/saliva (2.2 mg BSA) chambers was utilized to more accurately represent physiological transport conditions. All experimental conditions were identical between non-physiological and physiological experiments, except doses (67 μM and 284 μM), protein concentrations in media, and the final sample time of 32 h for the physiological experiment. Also, adding BSA to the media changed the pH slightly, from 7.4 to 7.2 for the plasma surrogate (basolateral media) but not the saliva surrogate media (7.4). The pH gradient was maintained throughout the physiological experiment. Since 2,4-D has a pKa of 2.73, pH values of media in both transport experiments were not expected to alter the 2,4-D ionization state or affect the resulting 2,4-D transport rate.

The basolateral to apical transfer of 2,4-D in the physiological media was much slower with the plasma to saliva protein gradient (Fig. 6A and B). Although 2,4-D was measured in the apical compartments as early as 2 h after dosing, the equilibrium point was not reached until after 24 h; where equilibrium was achieved < 24 h in the non-physiological experiment. In the apical chamber, 2,4-D concentrations at 24 h were not significantly different than concentrations at 32 h ($p = 0.177$), suggesting that equilibrium had been reached at different concentrations in the apical and basolateral compartments. The overall slow transfer and equilibrium at different concentrations in the apical and basolateral compartments is consistent with our hypothesis regarding the effect of substantial 2,4-D protein binding.

Simluations of 2,4-D transport under physiological conditions were achieved using parameters optimized to non-physiological conditions. After applying protein binding parameters measured in physiological media (see *Protein binding*), simulations utlizing the permeability coefficient (0.033 cm/h) optimized under non-physiological conditions was able to reasonably predict 2,4-D transport data for both 2,4-D concentrations tested (Fig. 6). This observation suggests that 2,4-D permeability of cells under both physiological and non-physiological conditions were consistent, and protein binding was the main factor driving observed differences in 2,4-D transport.

3.6. Sensitivity analysis

Sensitive parameters within the cellular computational model were identified for non-physiological and physiological conditions, following a basolateral dose of the lower doses (60 and 67 μM 2,4-D, respectively). In non-physiological simulations, only permeation and partition coefficients were sensitive (Fig. 7A and B). In the apical chamber, these parameters were sensitive throughout 24 h; while in the basolateral chamber, sensitivities were initially minor but increased over time. Protein binding parameters (binding sites and k_d) had a minimal role in modeling 2,4-D concentrations in both apical (Fig. 7A) and basolateral (Fig. 7B) chambers, compared to partition and permeation coefficients, which is most likely due to the low amount of protein binding in non-physiological conditions (~14% and ~11% bound for 60 and 457 μM 2,4-D). Under physiological conditions, where a protein gradient is present, protein binding parameters in the basolateral compartment (with a higher protein content) became more important in modeling 2,4-D transport to the apical chamber. Partition and permeability coefficients were additionally significant parameters as well (Fig. 7C). Notably, no parameters were significantly sensitive in modeling 2,4-D concentrations in the basolateral chamber (Fig. 7D). Overall, partition and permeation coefficients were consistently sensitive parameters and basolateral protein binding parameters were particularly important under physiological conditions for projecting 2,4-D transport to the apical chamber.

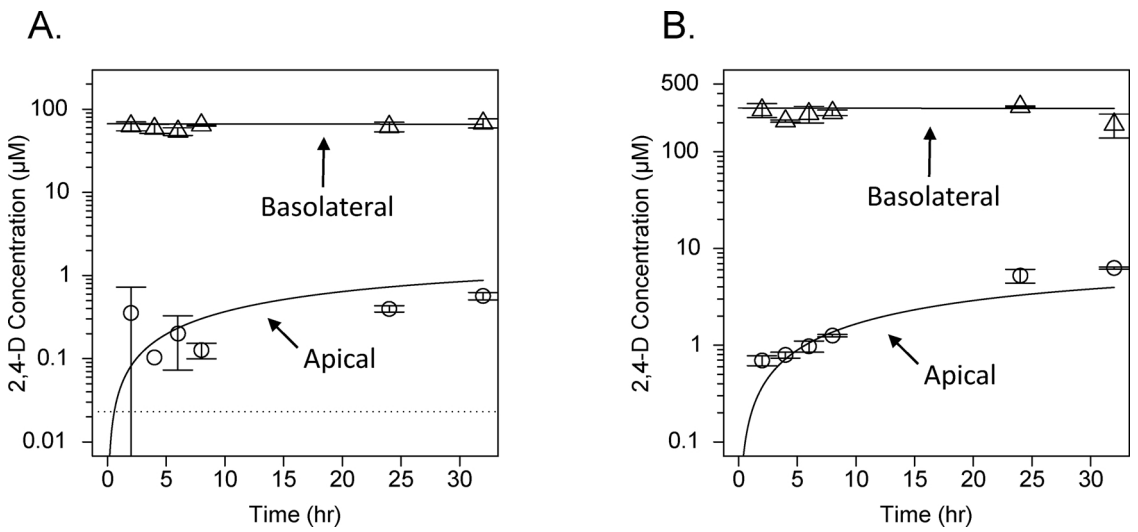

Fig. 6. Concentrations of 2,4-D in cell culture medium in the basolateral (triangles) and apical (circles) chambers over time after being dosed with 67 μM (A) or 284 μM (B) 2,4-D to the basolateral chamber under physiological experimental conditions. Lines are computational model simulations fit to the data. The dotted line represents the LOQ.

3.7. *In vivo* 2,4-D saliva clearance

Transport of 2,4-D into saliva was observed in rats following oral doses of 2,4-D. After administration of five different doses (30, 44, 67, 100, or 150 mg/kg) of 2,4-D, a non-linear protein binding response was observed in plasma over the specified dose range (Fig. 8A), indicating saturated protein binding and increased levels of free 2,4-D species at higher doses. Accordingly, a non-linear relationship between salivary and total plasma concentrations also resulted, notably demonstrating increased salivary 2,4-D concentrations at the highest dose (Fig. 8B). When comparing concentrations in saliva to unbound 2,4-D in plasma, a strong correlation was observed (Pearson correlation coefficient = 0.95, $p = 1.1 \times 10^{-7}$) (Fig. 8C), highlighting the impact of protein binding driving 2,4-D transport into saliva. Saliva/plasma (unbound) ratios (mean ± S.E.M; 0.0932 ± 0.0254) remained constant over all doses, while saliva/plasma (total) ratios (mean ± S.E.M; 0.0079 ± 0.0011) were only constant within the linear protein binding range. Overall, these results demonstrated *in vivo* 2,4-D transport into saliva at consistent levels (relative to plasma concentration) across doses below protein binding saturation, which is pivotal to assessing occupationally relevant exposures.

4. Discussion

2,4-D is currently widely applied in both large scale agricultural and residential settings and is expected to increase in use with the development of Enlist Duo™, a new technology benefiting from a mixture of 2,4-D and glyphosate herbicides (US EPA, 2017b). This phenoxy

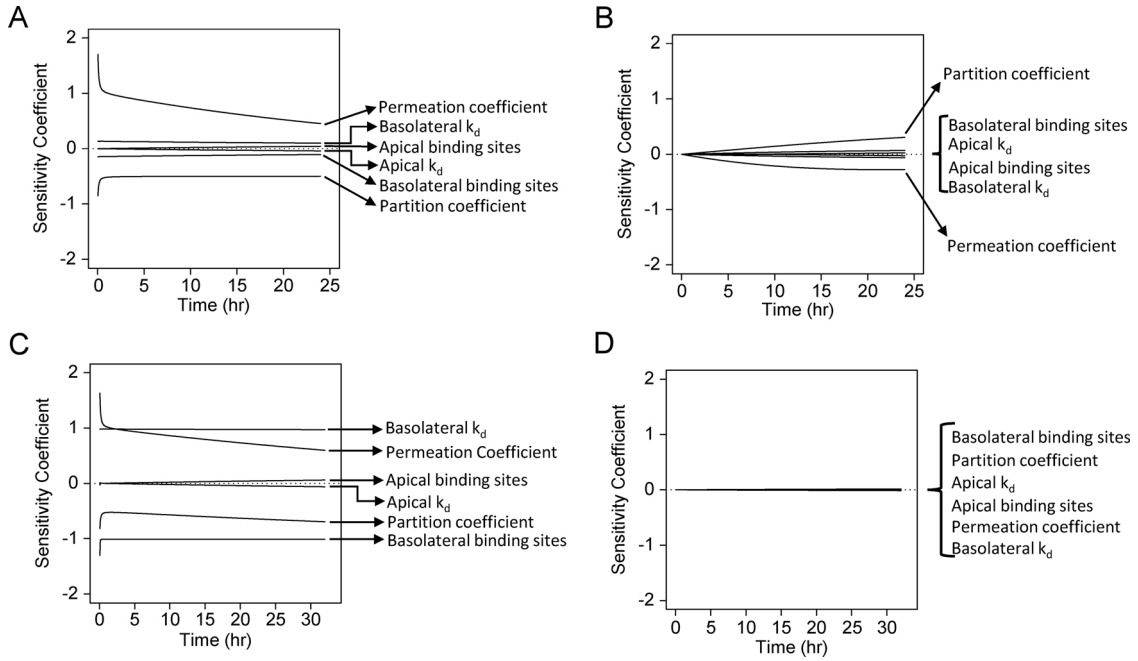

Fig. 7. Sensitivity coefficients of model parameters over time after simulating a 60 μM (non-physiological) or 67 μM (physiological) dose to the basolateral chamber. Parameters were assessed under non-physiological conditions in the apical (A) and basolateral (B) chambers, as well as under physiological conditions in the apical (C) and basolateral (D) chambers.

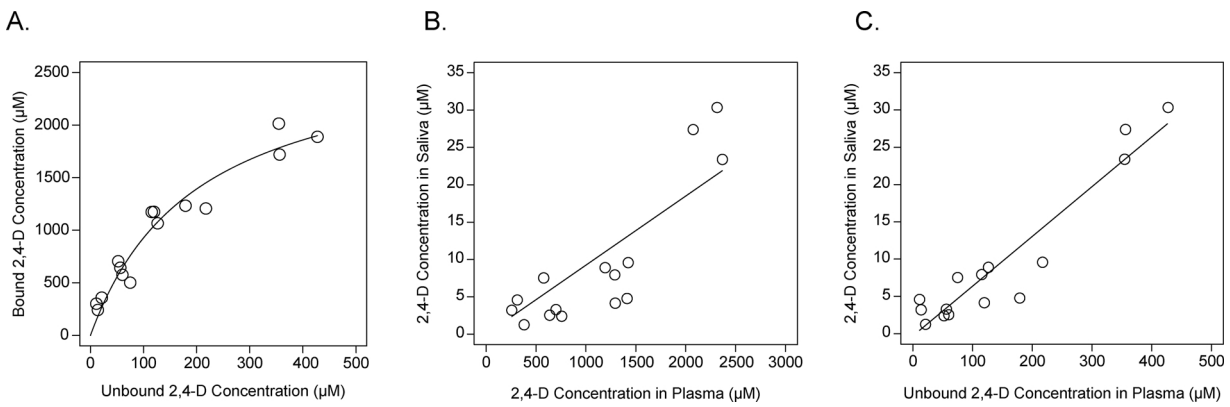

Fig. 8. Concentrations of 2,4-D in rat plasma and saliva following oral administration (30–150 mg/kg). Bound and unbound 2,4-D to proteins in plasma (A), correlation between salivary and total concentration in plasma (B) and correlation between salivary and unbound concentration in plasma (C).

herbicide has been in our environment for the past 70 years, and numerous studies have been conducted including pharmacokinetic, toxicity, environmental measurements, and human health impact studies, yet there remains important gaps in knowledge. First, there is a general lack of biomonitoring data for 2,4-D. Due to the rapidly increasing number of chemicals in our environment, biomonitoring has been advocated to provide accurate internal exposure dosimetry of environmental contaminants (Tox testing 21st century). Many epidemiologic investigations, reviews, or meta-analysis studies are limited by incomplete information. Less than a third of studies investigating pesticide exposures in farmworkers provide biomonitoring data (Quandt et al., 2006). Questionnaire based exposure classification, with or without algorithms to estimate the relative intensity of exposure, is prone to error and misclassification (Burns and Swaen, 2012; Thomas et al., 2010). The second knowledge gap concerns uncertainty from urinary biomonitoring. There are methods to evaluate 2,4-D exposures from urinary measurements, but levels of 2,4-D in urine represent total exposure over a specific time interval that do not correlate to blood or target-tissue concentrations. Furthermore, several studies have found high seasonal and intra-individual variability in urinary 2,4-D concentrations in pesticide applicators (Harris et al., 2010). This implies that there is day-to-day variability in 2,4-D exposures and single spot samples, 12 h, or even 24 h samples (despite creatinine adjustment) that may not portray 2,4-D exposures accurately. Even when resources are available for larger-scale biomonitoring, incomplete urinary collection or noncompliance can result in exclusion of over half of experimental subjects (Scher et al., 2008). Considering the seasonal use of 2,4-D and its short half-life (10–33 h), it may be beneficial to explore different methods of biofluid sampling and measurement in order to appropriately capture dose and time dependent exposures.

The purpose of this study was to evaluate the potential for non-invasive biomonitoring of 2,4-D in saliva. There are few data investigating salivary clearance of highly protein bound chemicals or weak acids, and as a result, their clearance is not well understood (Michalke et al., 2015). This study is the first to investigate the salivary clearance of 2,4-D, fulfilling a critical research gap. A previously established rat *in vitro* salivary system was used to investigate the transport mechanism of 2,4-D from plasma into saliva and further predict dose-dependent concentrations by modifying a recently developed computational model assessing pesticide transport into saliva (Smith et al., 2017; Timchalk et al., 2015; Weber et al., 2017). The transport of 2,4-D, a highly ionized organic acid, across the SGEC monolayer was predominantly driven by passive diffusion. 2,4-D is also highly protein bound (96–99%), and its relatively slow transfer across SGECs agreed with the hypothesis that a lower unbound fraction is available for diffusion. The *in vitro* partitioning, permeability, and protein binding kinetics of 2,4-D with a physiological protein gradient (simulating protein concentrations in plasma and saliva), were collectively predictive of salivary clearance. This approach emphasized the importance of protein binding to the overall transport kinetics of 2,4-D.

2,4-D transport to saliva appears to be dominated by passive diffusion both *in vitro* and *in vivo*. Transport of 2,4-D across SGECs did not display any saturable characteristics and was consistent regardless of the direction (basolateral to apical or *vice versa*) (Fig. 4A), suggesting passive diffusion as the primary mechanism. In addition, 2,4-D transfer was not affected by competition with a renal OAT substrate, PAH, in an *in vitro* system that forms polarized monolayers (Fig. 4B). In rats, saliva:plasma ratios were consistent within the linear protein binding range, indicitive of passive or non-saturable transport (Fig. 8B and C). These observations agree with other studies, where the majority of chemicals that are measured in saliva are understood to be cleared through passive diffusion and correspondingly display consistent and robust saliva/plasma ratios (Höld et al., 1996; Jusko and Gretch, 1976; Michalke et al., 2015). While the transfer of 2,4-D across SGECs and salivary clearance in rats adds strength to passive diffusion acting as the primary transport mechanism in the salivary clearance of 2,4-D, it is, however, not clear whether passive transcellular transfer or paracellular ultrafiltration predominates. Small (MW ~ ≤ 300 Da), hydrophilic molecules, such as 2,4-D (MW = 221.4 Da), can transfer through tight junctions by the paracellular route (Höld et al., 1996; Timchalk et al., 2015).

Overall, 2,4-D transport across the acinar monolayer was relatively slow when compared to the lipophilic metabolite of chlorpyrifos, TCPy, and is consistent with physiochemical and protein binding differences. Compared to 2,4-D, Smith et al. (2017) observed a lower maximum binding capacity but a higher affinity constant for TCPy. The substantial difference in the total number of binding sites between the two compounds may reflect an ability of 2,4-D to bind to a high capacity site, such as site II on albumin (Jusko and Gretch, 1976; Urien et al., 1996; Zhang et al., 2012). Furthermore, a lower physiological permeation coefficient across SGECs for 2,4-D (0.033 cm/h), compared to the permeation coefficient for TCPy (0.41 cm/h) (Smith et al., 2017), contributed to the slower transport of 2,4-D. Both 2,4-D and TCPy demonstrated dose-dependent times to reach equilibrium that is consistent with only the unbound fraction of pesticide or metabolite diffusing across the acinar monolayer. Notably, numerous investigations have demonstrated that protein binding characteristics strongly influence chemical transport, specifically salivary clearance (Angerer et al., 2007; Haeckel, 1993; Pichini et al., 1996; Smith et al., 2017). Sensitivity analyses of the cellular computational model also supported the importance of protein binding parameters, particularly when a protein gradient was present under physiological conditions (Fig. 7A–D).

Unlike TCPy, the SGECs did not predict *in vivo* saliva:plasma ratio for 2,4-D in rats. The average saliva:plasma (apical/basolateral) ratio *in vitro* (0.034) was significantly higher than the observed average ratio *in*

vivo (0.0079). We hypothesize that the lower *in vivo* ratio may be due to 2,4-D concentrations in saliva not being at equilibrium with 2,4-D concentrations in blood due to a higher permeation coefficient of 2,4-D compared to TCPy (Smith et al., 2017). Other physiological elements not present in the cell culture system (*e.g.* salivary and blood flow) may also contribute to the nonconcordant *in vitro* and *in vivo* saliva:plasma ratios. Salivary transport computational models (*e.g.* physiologically based pharmacokinetic (PBPK) models) could assess contributions of these physiological elements, along with the influence of other *in vivo* processes not found in cell culture systems (*e.g.* salivary and blood flow).

These findings provided a foundation for future investigations exploring 2,4-D detection in biological matrices, as well as understanding the pharmacokinetics that dictate detection limits. A comprehensive PBPK model with the flexibility to include physiological parameters of relevance (*e.g.* human *versus* rat model) offers insight regarding temporal and concentration constraints of detecting 2,4-D in various biological matrices. Extensive pharmacokinetic (Timchalk, 2004; Sauerhoff et al., 1977) and metabolomic (Van Ravenzwaay et al., 2003) assessments have been conducted, and PBPK models for 2,4-D (Kim et al., 1994; Durkin et al., 2004) have been developed, but an update of current models that incorporate salivary clearance will allow for quantitative interpretation of non-invasive salivary biomonitoring. These types of quantitative models could also promote development and application of field deployable 2,4-D sensors (Wang et al., 2017) and allow for rapid exposure assessment, particularly among those exposed occupationally.

5. Conclusions

This work highlighted the importance of protein binding in transport studies, specifically the use of physiologically relevant protein levels and computational modeling to understand the most influential predictors of transport, identified by parameter sensitivity analysis. The potential of 2,4-D for human biomonitoring was demonstrated in this study, but more data is needed to understand exposure levels from occupational settings. Saliva is a convenient, non-invasive matrix that may reflect unbound tissue levels and provide more information regarding blood concentrations. If critical pharmacokinetic parameters are known saliva could also offer more insight into free (and therefore the biologically active) chemical concentrations (Angerer et al., 2007; Pichini et al., 1996). Overall, we demonstrated that a weak acid (2,4-D) with high protein binding affinity is transported into saliva using both *in vitro* and *in vivo* models. Further work is needed to understand whether current sensor limits of detection are sufficient to measure occupationally relevant exposures.

Conflict of interest

The authors declare no conflicts of interest.

Acknowledgements

Authors would like to acknowledge Jamie Madden and Yunying Li for their support during *in vivo* experiments. This work was supported by CDC/NIOSH [grant numbers R01 OH008173 and R01 OH011023].

References

Aijaz, S., Balda, M.S., Matter, K., 2006. Tight junctions: molecular architecture and function. Int. Rev. Cytol. 248, 261–298.
Angerer, J., Ewers, U., Wilhelm, M., 2007. Human biomonitoring: state of the art. Int. J. Hyg. Environ. Health 210, 201–228.
Arcury, T.A., Quandt, S.A., Barr, D.B., Hoppin, J.A., McCauley, L., Grzywacz, J.G., Robson, M.G., 2006. Farmworker exposure to pesticides: methodologic issues for the collection of comparable data. Environ. Health Perspect. 923–928.
Aylward, L.L., Hays, S.M., 2008. Biomonitoring equivalents (BE) dossier for 2,4-dichlorophenoxyacetic acid (2,4-D) (CAS No. 94-75-7). Regul. Toxicol. Pharmacol. 51, S37–48.
Aylward, L.L., Morgan, M.K., Arbuckle, T.E., Barr, D.B., Burns, C.J., Alexander, B.H., Hays, S.M., 2010. Biomonitoring data for 2,4-dichlorophenoxyacetic acid in the United States and Canada: interpretation in a public health risk assessment context using Biomonitoring Equivalents. Environ. Health Perspect. 118, 177–181.
Aylward, L.L., Kirman, C.R., Schoeny, R., Portier, C.J., Hays, S.M., 2013. Evaluation of biomonitoring data from the CDC National Exposure Report in a risk assessment context: perspectives across chemicals. Environ. Health Perspect. 121, 287–294.
Bulgakova, N.A., Knust, E., 2009. The crumbs complex: from epithelial-cell polarity to retinal degeneration. J. Cell Sci. 122, 2587–2596.
Burns, C.J., Swaen, G.M., 2012. Review of 2,4-dichlorophenoxyacetic acid (2,4-D) biomonitoring and epidemiology. Crit. Rev. Toxicol. 42, 768–786.
Caporossi, L., Santoro, A., Papaleo, B., 2010. Saliva as an analytical matrix: state of the art and application for biomonitoring. Biomarkers 15, 475–487.
Carpenter, G.H., 2013. The secretion, components, and properties of saliva. Annu. Rev. Food Sci. Technol. 4, 267–276.
Charles, J.M., Cunny, H.C., Wilson, R.D., Bus, J.S., 1996. Comparative subchronic studies on 2,4-dichlorophenoxyacetic acid, amine, and ester in rats. Fundam. Appl. Toxicol. 33, 161–165.
Durkin, P., Hertzberg, R., Diamond, G., 2004. Application of PBPK model for 2,4-D to estimates of risk in backpack applicators. Environ. Toxicol. Pharmacol. 16, 73–91.
Esteban, M., Castano, A., 2009. Non-invasive matrices in human biomonitoring: a review. Environ. Int. 35, 438–449.
Ferrari, M., Negri, S., Zadra, P., Ghittori, S., Imbriani, M., 2008. Saliva as an analytical tool to measure occupational exposure to toluene. Int. Arch. Occup. Environ. Health 81, 1021–1028.
Garabrant, D.H., Philbert, M.A., 2002. Review of 2,4-dichlorophenoxyacetic acid (2,4-D) epidemiology and toxicology. Crit. Rev. Toxicol. 32, 233–257.
Goodman, J.E., Loftus, C.T., Zu, K., 2015. 2,4-Dichlorophenoxyacetic acid and non-Hodgkin's lymphoma, gastric cancer, and prostate cancer: meta-analyses of the published literature. Ann. Epidemiol. 25, 626–636 e624.
Grover, R., Cessna, A.J., Muir, N.I., Riedel, D., Franklin, C.A., Yoshida, K., 1986. Factors affecting the exposure of ground-rig applicators to 2,4-D dimethylamine salt. Arch. Environ. Contam. Toxicol. 15, 677–686.
Haeckel, R., 1993. Factors influencing the saliva/plasma ratio of drugs. Ann. N. Y. Acad. Sci. 694, 128–142.
Harris, S.A., Villeneuve, P.J., Crawley, C.D., Mays, J.E., Yeary, R.A., Hurto, K.A., Meeker, J.D., 2010. National study of exposure to pesticides among professional applicators: an investigation based on urinary biomarkers. J. Agric. Food Chem. 58, 10253–10261.
Hidalgo, I.J., Raub, T.J., Borchardt, R.T., 1989. Characterization of the human colon carcinoma cell line (Caco-2) as a model system for intestinal epithelial permeability. Gastroenterology 96, 736–749.
Hoar, S.K., Blair, A., Holmes, F.F., Boysen, C.D., Robel, R.J., Hoover, R., Fraumeni Jr., J.F., 1986. Agricultural herbicide use and risk of lymphoma and soft-tissue sarcoma. JAMA 256, 1141–1147.
Höld, K.M., de Boer, D., Zuidema, J., Maes, R.A.A., 1996. Saliva as an analytical tool in toxicology. Int. J. Drug Test 1, 1–36.
Humphrey, S.P., Williamson, R.T., 2001. A review of saliva: normal composition, flow, and function. J. Prosthet. Dent. 85, 162–169.
Jusko, W.J., Gretch, M., 1976. Plasma and tissue protein binding of drugs in pharmacokinetics. Drug Metab. Rev. 5, 43–140.
Jusko, W.J., Milsap, R.L., 1993. Pharmacokinetic principles of drug distribution in saliva. Ann. N. Y. Acad. Sci. 694, 36–47.
Kaufman, E., Lamster, I.B., 2002. The diagnostic applications of saliva–a review. Crit. Rev. Oral Biol. Med. 13, 197–212.
Kennepohl, E., et al., 2010. Chapter 84 – phenoxy herbicides (2,4-D) A2 - Krieger, Robert. Hayes' Handbook of Pesticide Toxicology, third edition. Academic Press, New York, pp. 1829–1847.
Kim, C.S., Gargas, M.L., Andersen, M.E., 1994. Pharmacokinetic modeling of 2,4-dichlorophenoxyacetic acid (2,4-D) in rat and in rabbit brain following single dose. Toxicol. Lett. 74, 189–201.
Lew, K., Acker, J.P., Gabos, S., Le, X.C., 2010. Biomonitoring of arsenic in urine and saliva of children playing on playgrounds constructed from chromated copper arsenate-treated wood. Environ. Sci. Technol. 44, 3986–3991.
Lu, C., 2006. Using salivary biomarker for pesticide exposure and risk assessment: possibilities and pitfalls. Epidemiology 17, S135.
Michalke, B., Rossbach, B., Goen, T., Schaferhenrich, A., Scherer, G., 2015. Saliva as a matrix for human biomonitoring in occupational and environmental medicine. Int. Arch. Occup. Environ. Health 88, 1–44.
Mironov, G.G., Okhonin, V., Gorelsky, S.I., Berezovski, M.V., 2011. Revealing equilibrium and rate constants of weak and fast noncovalent interactions. Anal. Chem. 83, 2364–2370.
Moy, T.W., Brumley, W.C., 2003. Multiresidue determination of acidic pesticides in water by HPLC-DAD with confirmation by GC-MS using conversion to the methyl ester with trimethylsilyldiazomethane. J. Chromatogr. Sci. 41, 343–349.
Munro, I.C., Carlo, G.L., Orr, J.C., Sund, K.G., Wilson, R.M., Kennepohl, E., Lynch, B.S., Jablinske, M., 1992. A comprehensive, integrated review and evaluation of the scientific evidence relating to the safety of the herbicide 2, 4-D. Int. J. Toxicol. 11, 559–664.
Pichini, S., Altieri, I., Zuccaro, P., Pacifici, R., 1996. Drug monitoring in nonconventional biological fluids and matrices. Clin. Pharmacokinet. 30, 211–228.
Quandt, S.A., Hernandez-Valero, M.A., Grzywacz, J.G., Hovey, J.D., Gonzales, M., Arcury, T.A., 2006. Workplace, household, and personal predictors of pesticide exposure for farmworkers. Environ. Health Perspect. 114, 943–952.

Ranz, A., Maier, E., Motter, H., Lankmayr, E., 2008. Extraction and derivatization of polar herbicides for GC-MS analyses. J. Sep. Sci. 31, 3021–3029.
Sauerhoff, M.W., Braun, W.H., Blau, G.E., Gehring, P.J., 1977. The fate of 2,4-dichlorophenoxyacetic acid (2,4-D) following oral administration to man. Toxicology 8, 3–11.
Scher, D.P., Sawchuk, R.J., Alexander, B.H., Adgate, J.L., 2008. Estimating absorbed dose of pesticides in a field setting using biomonitoring data and pharmacokinetic models. J. Toxicol. Environ. Health A 71, 373–383.
Silva, M.J., Reidy, J.A., Samandar, E., Herbert, A.R., Needham, L.L., Calafat, A.M., 2005. Detection of phthalate metabolites in human saliva. Arch. Toxicol. 79, 647–652.
Smith, J.N., Wang, J., Lin, Y., Timchalk, C., 2010. Pharmacokinetics of the chlorpyrifos metabolite 3,5,6-trichloro-2-pyridinol (TCPy) in rat saliva. Toxicol. Sci. 113, 315–325.
Smith, J.N., Wang, J., Lin, Y., Klohe, E.M., Timchalk, C., 2012. Pharmacokinetics and pharmacodynamics of chlorpyrifos and 3,5,6-trichloro-2-pyridinol in rat saliva after chlorpyrifos administration. Toxicol. Sci. 130, 245–256.
Smith, J.N., Carver, Z.A., Weber, T.J., Timchalk, C., 2017. Predicting transport of 3,5,6-trichloro-2-Pyridinol into saliva using a combination experimental and computational approach. Toxicol. Sci. 157, 438–450.
Smolders, R., Schramm, K.W., Nickmilder, M., Schoeters, G., 2009. Applicability of non-invasively collected matrices for human biomonitoring. Environ. Health 8, 8.
Staff, J.F., Harding, A.H., Morton, J., Jones, K., Guice, E.A., McCormick, T., 2014. Investigation of saliva as an alternative matrix to blood for the biological monitoring of inorganic lead. Toxicol. Lett. 231, 270–276.
Thomas, K.W., Dosemeci, M., Coble, J.B., Hoppin, J.A., Sheldon, L.S., Chapa, G., Croghan, C.W., Jones, P.A., Knott, C.E., Lynch, C.F., Sandler, D.P., Blair, A.E., Alavanja, M.C., 2010. Assessing a pesticide exposure intensity algorithm in the agricultural health study. J. Expo. Sci. Environ. Epidemiol. 20, 559–569.
Timchalk, C., 2004. Comparative inter-species pharmacokinetics of phenoxyacetic acid herbicides and related organic acids. Evidence that the dog is not a relevant species for evaluation of human health risk. Toxicology 200, 1–19.
Timchalk, C., Weber, T.J., Smith, J.N., 2015. Computational strategy for quantifying human pesticide exposure based upon a saliva measurement. Front. Pharmacol. 6, 115.
Urien, S., Barre, J., Morin, C., Paccaly, A., Montay, G., Tillement, J.P., 1996. Docetaxel serum protein binding with high affinity to alpha 1-acid glycoprotein. Invest. New Drugs 14, 147–151.
US EPA, 2017a. Pesticides Industry Sales and Usage: 2008 - 2012 Market Estimates. Office of Chemical Safety and Pollution Prevention. EPA.
US EPA, 2017b. Registration of Enlist Duo|US EPA. [online] Available at:. (Accessed 30 March 2018). https://www.epa.gov/ingredients-used-pesticide-products/registration-enlist-duo.
van Ravenzwaay, B., Hardwick, T.D., Needham, D., Pethen, S., Lappin, G.J., 2003. Comparative metabolism of 2,4-dichlorophenoxyacetic acid (2,4-D) in rat and dog. Xenobiotica 33, 805–821.
Villalobos, A.R., Dunnick, C.A., Pritchard, J.B., 1996. Mechanism mediating basolateral transport of 2,4-dichlorophenoxyacetic acid in rat kidney. J. Pharmacol. Exp. Ther. 278, 582–589.
von Stackelberg, K., 2013. A systematic review of carcinogenic outcomes and potential mechanisms from exposure to 2,4-D and MCPA in the environment. J. Toxicol. 2013, 371610.
Wang, Y., Zeinhom, M.M.A., Yang, M., Sun, R., Wang, S., Smith, J.N., Timchalk, C., Li, L., Lin, Y., Du, D., 2017. A 3D-Printed, portable, optical-sensing platform for smartphones capable of detecting the herbicide 2,4-Dichlorophenoxyacetic acid. Anal. Chem. 89, 9339–9346.
Weber, T.J., Smith, J.N., Carver, Z.A., Timchalk, C., 2017. Non-invasive saliva human biomonitoring: development of an in vitro platform. J. Expo. Sci. Environ. Epidemiol. 27, 72–77.
Zahm, S.H., Weisenburger, D.D., Babbitt, P.A., Saal, R.C., Vaught, J.B., Cantor, K.P., Blair, A., 1990. A case-control study of non-Hodgkin's lymphoma and the herbicide 2,4-dichlorophenoxyacetic acid (2,4-D) in eastern Nebraska. Epidemiology 1, 349–356.
Zhang, F., Xue, J., Shao, J., Jia, L., 2012. Compilation of 222 drugs' plasma protein binding data and guidance for study designs. Drug Discov. Today 17, 475–485.